

Micro sensor for determination of thin layer thickness and refractive index

Martin Schädel, Dennis Mitrenga, Philip Schmitt, Andreas T. Winzer
and Olaf Brodersen

CiS Forschungsinstitut für Mikrosensorik und Photovoltaik GmbH,
Konrad-Zuse-Str. 14, 99099 Erfurt, Germany

Abstract We present a microoptical sensor solution for measuring thicknesses and refractive indices of thin layers by measuring changes in polarization of two laser beams under inclined angle of incidence. The compact architecture does not require any moving or rotating components and allows for low-maintenance and robust operation. The measured polarized reflection is modelled by Transfer Matrix method and Levenberg-Marquard fit algorithms in order to obtain the target sample characteristics. Single layer samples of SiO_2 , SiO_xN_y and SiN_x on Silicon substrate were analyzed. For several different single layer systems the deviations of layer thicknesses and refractive indices are below 3% as compared to independent reference measurements.

1 Introduction

The characterization of sample surfaces and thin coating layers by measuring changes in light polarization is a rather old discipline. The fundamental relations of light polarization, material properties and sample architecture can be described by Maxwell and Fresnel equations. Today many elaborated measuring techniques base upon these fundamentals, for example spectral or laser ellipsometry or reflectometry [1]. In order to obtain universally applicable and high precision instruments, the complexity of these setups is rather high. Most of the common instruments using rotating optical components (e.g. polarizers), monochromators or CCD elements [2], causing rather large setups with high alignment effort. On the other hand the increasing degree of automation in

production processes requires monitoring and control of product properties in a rather small parameter range. For this scenario high precision laboratory instruments are often overdimensioned. Here small, robust and fast measuring heads are often sufficient and allow for easy integration into production lines and price-conscious monitoring units.

We present a compact sensor that measures the polarized reflection for two wavelengths and operates without any moving or rotating components. The device can be used to determine the optical properties (refractive index) and film thickness of thin surface layers.

We start with a brief description of the theoretical background, including the Transfer-Matrix-Method for multi-layer thin film coatings. This method is used to model the experimental data by Levenberg-Marquardt fit routines. The device architecture and working principle is described in the third section. Experimental results are discussed and compared with independently analyzed reference samples in section four, followed by a summary and outlook.

2 Theoretical Background

The consideration of Maxwells equation at an interface of two isotropic materials leads to Snell's law and Fresnel equations for the description of electric fields amplitudes and phases [3]. The impact of the interface can be written in form of a matrix [2]:

$$\begin{pmatrix} \underline{E}_{m,i} \\ \underline{E}_{m,r} \end{pmatrix} = \frac{1}{t_m} \begin{pmatrix} 1 & r_m \\ r_m & 1 \end{pmatrix} \begin{pmatrix} \underline{E}_{m,t} \\ \underline{E}_{m,b} \end{pmatrix} = I_m \begin{pmatrix} \underline{E}_{m,t} \\ \underline{E}_{m,b} \end{pmatrix} \quad (20.1)$$

where the \underline{E} are the complex electric fields at the interface m of the incoming (index i), reflected (index r), transmitted (index t) and back reflected light of subsequent interfaces in the layer stack (index b). t_m and r_m are the Fresnel coefficients for transmission and reflection, respectively. Both are functions of the refractive indices at the interface and thus in general depend on wavelength. I_m is called the interface matrix of interface m . For isotropic materials, the parallel and perpendicular fractions of light can be treated independently. Thus I_m is obtained for both cases by using the corresponding Fresnel equations.

The passage of a layer with thickness d_m has impact on the amplitude and phase of the electric field and can also be written in form of a matrix

[2]:

$$\begin{pmatrix} \underline{E}_{m,t} \\ \underline{E}_{m,b} \end{pmatrix} = \begin{pmatrix} e^{i\beta_m d_m} & 0 \\ 0 & e^{-i\beta_m d_m} \end{pmatrix} \begin{pmatrix} \underline{E}_{m+1,i} \\ \underline{E}_{m+1,r} \end{pmatrix} = L_m \begin{pmatrix} \underline{E}_{m+1,i} \\ \underline{E}_{m+1,r} \end{pmatrix} \quad (20.2)$$

with:

$$\beta_m = \frac{2\pi}{\lambda} \underline{N}_m \cos \underline{\phi}_m \quad , \quad (20.3)$$

the layer thickness d_m and the complex refractive index $\underline{N}_m = n_m + ik_m$, wherein n_m is the refractive index and k_m is the extinction coefficient of layer m . Both material properties depend on the wavelength λ . L_m is called the layer matrix of layer m and $\underline{\phi}_m$ is the complex angle of light propagation within the layer m , calculated by Snell's law.

Using the previous equations a layer system with M layers can be written as [2]:

$$\begin{aligned} \begin{pmatrix} \underline{E}_i \\ \underline{E}_r \end{pmatrix} &= I_1 L_1 I_2 L_2 \dots I_M L_M I_{M+1} \begin{pmatrix} \underline{E}_t \\ 0 \end{pmatrix} \\ &= \prod_{m=1}^M (I_m L_m) I_{M+1} \begin{pmatrix} \underline{E}_t \\ 0 \end{pmatrix} \\ &= P \begin{pmatrix} \underline{E}_t \\ 0 \end{pmatrix} = \begin{pmatrix} P_{11} & P_{12} \\ P_{21} & P_{22} \end{pmatrix} \begin{pmatrix} \underline{E}_t \\ 0 \end{pmatrix} \quad . \end{aligned} \quad (20.4)$$

P is the transfer matrix of the stacked layer system. The equation can be used to calculate the total external reflected (\underline{E}_r) and transmitted (\underline{E}_t) electric fields for a given \underline{E}_i . In order to express coefficients for reflected light intensities, the real part of the Poynting vector is used and leads to:

$$R = \frac{S_r}{S_i} = \frac{|\underline{E}_r|^2}{|\underline{E}_i|^2} = \frac{|P_{21}|^2}{|P_{11}|^2}, \quad (20.5)$$

where S_r and S_i are the light intensities (in Wm^{-2}) of the reflected and incidence light, respectively. Eq. 20.5 can be used to calculate the parallel and perpendicular reflection for different wavelengths by changing λ in Eq.20.3 and using the corresponding Fresnel coefficients in Eq.20.1 for each layer in the system.

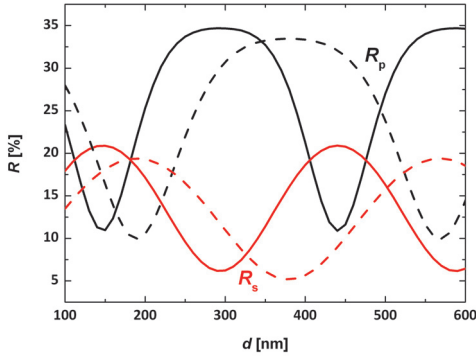


Figure 20.1: Simulated reflectance of a SiO_2 film ($n(660\text{ nm}) = 1.4563$; $n(850\text{ nm}) = 1.4525$) on Silicon substrate using a wavelength of 660 nm (solid) and 850 nm (dashed) with parallel (black) and perpendicular (red) polarization

With the previous equations the reflection coefficients of parallel and perpendicular light intensity can be calculated for any (isotropic) layer system. In reverse the equations can be used to find unknown sample properties by fitting the layer properties on experimental data of R_p and R_s . A common fitting routine (for example often applied in fitting spectral ellipsometry data) is the Levenberg-Marquard routine, that combines the Gradient Method and the Hesse Matrix Method in order to find the best agreement of experimental and modelled data in a multi parameter space [4]. For our software we used the figure of merit (FOM) as a measure for the model agreement with experimental data, as it takes into account the individual uncertainties of the measured values [5].

Using a single wavelength allows for two measurable values and thus for modelling up to two independent sample attributes, for example d and n of a transparent surface layer on top of a known substrate. However using only one wavelength has two mayor limitations: first the results of R_p and R_s are periodic in the parameter space, and second the sensitivity on the tested parameter might be very low, depending on the actual sample architecture.

These limitations are illustrated in Fig.20.1 for the example of a SiO_2 film with unknown layer thickness on a silicon substrate. Consider a single wavelength (for example the sold lines in Fig.20.1 for 660 nm) a periodic change in both R_p and R_s with layer thickness is obvious, showing several possible results of d for the same values of R_p and R_s . Thus no unique fit result for the unknown layer thickness is obtained with a single wavelength (unless the sample attribute is already well known and only a small parameter range is allowed in the fit). The second limitation of low parameter sensitivity is obvious in the area of local extrema, where the slopes of R_p and R_s are very small. In this area large changes in d causes only small changes of the measurable reflection. As the measured values will have uncertainties, the modelled parameter will have a rather large uncertainty in this region as well.

In order to overcome these disadvantages, a second wavelength can be applied. As illustrated in Fig.20.1 the additional information allows for unique fit results and increases the model sensitivity on the tested parameter, because at least one of the measured values shows a steep slope in the parameter space.

3 Sensor Architecture

The previous considerations made clear that the sensor requires more than a single wavelength setup. In order to obtain high sensitivity and unique fit results additional information is required, for example by multiple angles of incidence or a second wavelength. We decided for the latter. A schematic of the setup is shown in Fig.20.2 together with a photography of a first demonstrator setup of the optical subunit of the sensor. This unit is controlled by demonstrator electronics and placed in a 3D-printed housing with three adjustable feet for tilt alignment, as shown in Fig.20.3. The components are described in detail in the following sections.

3.1 Micro Optical Laser Source Unit

We chose a wafer based approach in order to achieve a high degree of miniaturization and a technology suitable for a large number of pieces. A low cost - high precision solution is the polymer-on-glass (POG) tech-

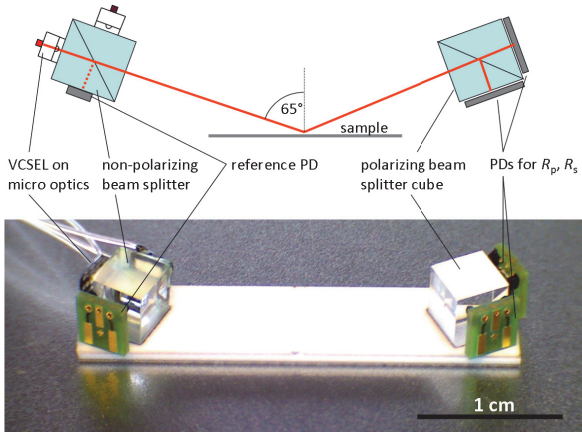


Figure 20.2: Schematic illustration and photography of a populated ceramic holder, including a two-wavelength laser source cube on the left, and a polarization detector cube on the right.

nology, see for instance [6]. Supported by optical simulations a $1100 \times 700 \times 640 \mu\text{m}^3$ micro optic was designed. The optics includes a glass wafer with a polymer lens and a polymer spacer at the front, and a lithographically structured thin film metal contact at the back side. The metal acts as an aperture as well as the front contact of the VCSEL (vertical cavity surface emitting laser). The $240 \times 240 \mu\text{m}^2$ VCSEL chips were soldered “face down” onto the metal side of the optics wafer. The apertures of the VCSEL chips and those of the optics wafer were aligned to each other. After that, the micro optics were tested for laser beam quality and subsequently diced into individual units. The micro optic laser source achieves spot sizes below $300 \mu\text{m}$ at the measurement distance.

Two laser units were used for the sensor. Each equipped with single mode VCSEL chip of 670 nm and 850 nm wavelength, respectively. They were mounted on the two entrance sides of a 50:50 beam splitter. Active 5-axis alignment was used together with an on-axis beam profiling camera and a rotating polarizing filter. This ensured the same optical axis and the target orientation of the linearly polarized laser light for both laser units. Since they showed a high degree of linear polarization ($> 98\%$) no additional polarizer is required within the sensor device.

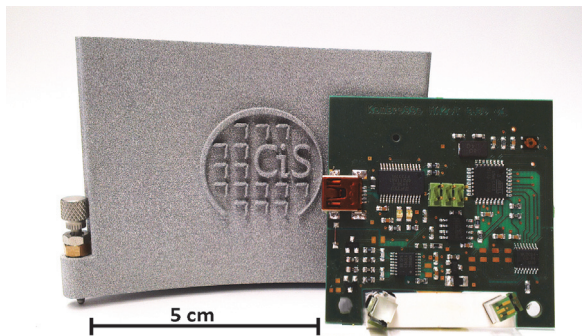


Figure 20.3: Photography of the demonstrator electronics equipped with the optical unit in front of the 3D printed housing.

On the second exit face of the beam splitter cube, a monitor photodiode was mounted. Its signal is used for monitoring and controlling the light intensity of the VCSELs.

3.2 Detector Unit

Two photo detectors were mounted on a second polarizing beam splitter cube (dielectric filter system, degree of polarization $> 10000:1$ for both wavelengths $\pm 10\text{ nm}$). As beam misalignment might be a topic in the later application of the sensor, two monolithic double photodiodes are applied. The detector for the parallel polarized part is tilted by 90° against the detector for the perpendicular component. The effect of this arrangement equals a classical 4-quadrant diode and allows for determination of errors in effective angle of incidence and possible light losses. For the application of the sensor in an automated measuring unit, this information can be used for readjustment of the sensor or the sample.

The source and detector units must be aligned according to the target angle of incidence on the sample's surface. As a good compromise between achievable accuracy in sensor alignment and sensitivity on sample attributes, we chose an angle of incidence of 65° . The source and

detector units are mounted on a ceramic holder in order to reduce mechanical stress for example due to temperature or moisture exposure. The ceramics were laser cut and exhibit edge guides for easier alignment of the source and detector beam splitter cubes. The alignment was performed with active source and detector units adjusted by a fixed reference mirror within the assembly tool and controlled by a beam profiling camera on the optical axis. A photography of the optical unit of a first sensor prototype is shown in Fig.20.2 together with a schematic of the setup.

Finally the populated ceramic holder was attached on an electronic board placed in a 3D printed sensor housing.

3.3 Electronics and Software

For the demonstrator a read out and driving circuit was designed and realized in a 5×5 cm² board. The circuit contains a micro controller, an AD-Converter and a DA-Converter to operate the VCSELs with constant current and to read out the amplified and AD converted (16 bit) signals of the photo detectors. The measurement procedure includes a dark measurement (to account for residual ambient light), a measurement with the red and the infrared VCSEL. Several measurements are performed, the mean value is corrected by the dark measurement and transferred to a PC via serial USB connection. The total procedure takes only 50 ms that allows for fast applications like scanning a sample surface or tracking the properties of a moving sample beneath the sensor head.

Measurement and data acquisition is triggered by a PC with a Lab-View software. The transfer matrix fitting routines are implemented and results of the fit parameters are reported together with confidence intervals and the correlation matrix.

4 Experimental Results

A set of reference samples with different dielectric layers on silicon substrates were fabricated by plasma enhanced chemical vapour deposition (PECVD). We choose SiO₂, SiO_xN_y and SiN_x in three different layer thicknesses each in order to obtain coatings with different refractive in-

dices. The $2 \times 2 \text{ cm}^2$ samples were analyzed in independent external laboratories by spectroscopic ellipsometry and reflectometry. The mean values of n and d of five measuring positions were used as reference for testing the new sensor.

The following results are obtained by a laboratory set up of the sensor. As electronic development is still in progress, a multi channel data acquisition module (NI 9215) was used instead of the sensor specific electronics described in the previous section. Each value is obtained by the average of five measured signals and their corresponding standard deviation. Measurements in the dark and on a blank Silicon sample were performed in order to calibrate light intensities. In combination with the measurements of the sample, R_p and R_s and their corresponding uncertainties are obtained for two wavelengths (670 nm and 850 nm). n and d are then modelled by Transfer-Matrix and Levenberg-Marquardt-Fitting routines.

In Fig. 20.4 the results for the reference samples are illustrated as a function of externally measured reference values. The obtained results with the new sensor are in good agreement with the reference values. The deviation is below 3% for all n and d except for the 200 nm SiN_x layer thickness, which is about 5%.

In addition experiments with two layer systems were performed. Accuracy and model sensitivity for the buried layer decreases significantly as compared to a single layer system. In case of well known attributes of the buried layer, the surface layer of the stack can be characterized with only small increase in deviation and confidence interval (deviation typically below 5%). Similar limitations can be observed for example with professional laser ellipsometers on double layer systems.

5 Summary

We presented the concept and the first results of a miniaturized sensor for reflective polarimetry. The device works with two single mode VCSELs (670 and 850 nm) in a micro optical unit with beam diameters below $300 \mu\text{m}$. The lasers are combined by a beam splitter cube and a monitor photo diode in order to obtain a stabilized two-colour laser source unit. The reflected light is detected under an angle of incidence of 65° by a polarization beam splitter cube equipped with photo detec-

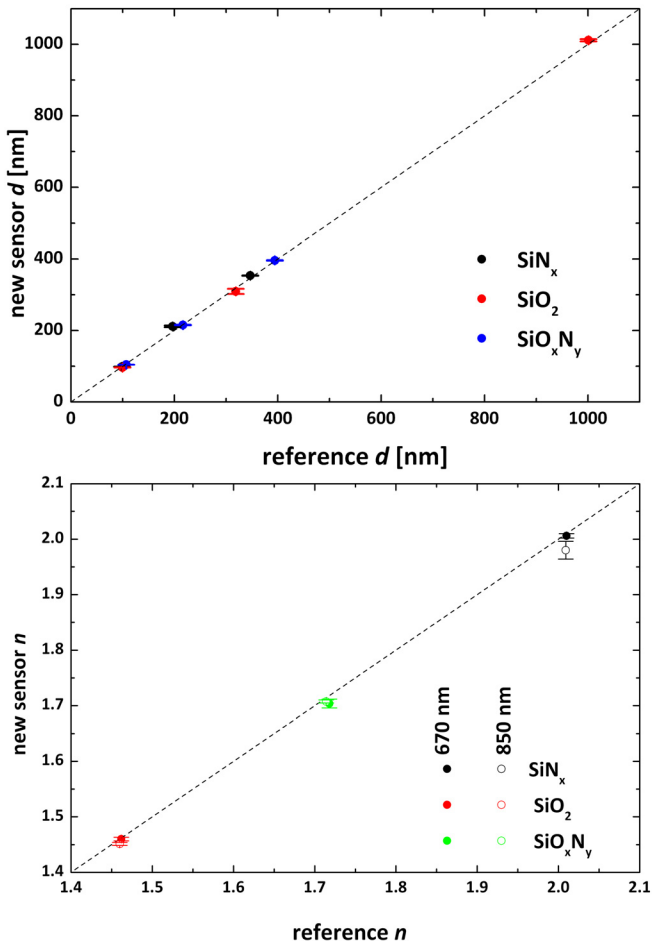


Figure 20.4: Experimental results as a function of externally measured reference values for layer thickness d and refractive index n for different dielectric layers and two wavelengths, indicated in the plots. Error bars indicate the confidence intervals of modelled results of the new sensor device.

tors. The sensor demonstrator is driven by an electronic unit, including AD conversion and serial communication with a PC. However the

electronic development is still in progress. A self-developed software is used to model the thickness and the refractive indices of a thin surface layer. As compared to external references a laboratory setup obtained typical deviations below 3% of layer thickness and refractive indices for SiO_2 , SiO_xN_y and SiN_x layers with thicknesses in the range of 100 to 1000 nm. Further improvement of the results is expected by application of the final electronics.

Acknowledgment

The development is financially supported by the German Federal Ministry of Economic Affairs and Energy (BMWi), program INNO-KOM-Ost (projects MF130023 and MF130021).

References

1. H. Tomkins and W. McGahan, *Spectroscopic Ellipsometry and Reflectometry*. John Wiley and Sons, Inc., 1999, ch. Appendix, pp. 222–224.
2. R. Azzam and N. Bashara, *Ellipsometry and Polarized Light*. North-Holland, Amsterdam, 1977.
3. J. Jackson, *Klassische Elektrodynamik*. Walter de Gruyter, 2002.
4. W. Press, S. Teukolsky, W. Vetterling, and B. Flannery, *Numerical Recipes in C++: The Art of Scientific Computing*, ser. 2nd edition. Cambridge University Press, 2002.
5. H. Tompkins and E. Irene, *Handbook of Ellipsometry*. 1. Auflage Springer, Berlin, 2006.
6. P. Dannberg, F. Wippermann, A. Brückner, A. Matthes, P. Schreiber, and A. Bräuer, "Wafer-level hybrid integration of complex micro-optical modules," *Micromachines*, vol. 5, no. 2, pp. 325–340, 2014. [Online]. Available: <http://www.mdpi.com/2072-666X/5/2/325>